Cell Death and Differentiation (2015) 22, 1517–1525

www.nature.com/cdd

The LIM-only transcription factor LMO2 determines tumorigenic and angiogenic traits in glioma stem cells

S-H Kim[1,2], E-J Kim[1], M Hitomi[3], S-Y Oh[1], X Jin[4], H-M Jeon[1], S Beck[5], X Jin[1], J-K Kim[1], CG Park[1], S-Y Chang[1], J Yin[6], T Kim[7], Y-j Jeon[8], J Song[2], YC Lim[9], JD Lathia[3,10,11], I Nakano[*,2,12] and H Kim[*,1]

Glioblastomas (GBMs) maintain their cellular heterogeneity with glioma stem cells (GSCs) producing a variety of tumor cell types. Here we interrogated the oncogenic roles of Lim domain only 2 (LMO2) in GBM and GSCs in mice and human. High expression of LMO2 was found in human patient-derived GSCs compared with the differentiated progeny cells. LMO2 is required for GSC proliferation both *in vitro* and *in vivo*, as shRNA-mediated LMO2 silencing attenuated tumor growth derived from human GSCs. Further, LMO2 is sufficient to induce stem cell characteristics (stemness) in mouse premalignant astrocytes, as forced LMO2 expression facilitated *in vitro* and *in vivo* growth of astrocytes derived from *Ink4a/Arf* null mice and acquisition of GSC phenotypes. A subset of mouse and human GSCs converted into vascular endothelial-like tumor cells both *in vitro* and *in vivo,* which phenotype was attenuated by LMO2 silencing and promoted by LMO2 overexpression. Mechanistically, the action of LMO2 for induction of glioma stemness is mediated by transcriptional regulation of Jagged1 resulting in activation of the Notch pathway, whereas LMO2 directly occupies the promoter regions of the VE-cadherin gene for a gain of endothelial cellular phenotype. Subsequently, selective ablation of human GSC-derived VE-cadherin-expressing cells attenuated vascular formation in mouse intracranial tumors, thereby significantly prolonging mouse survival. Clinically, LMO2 expression was elevated in GBM tissues and inversely correlated with prognosis of GBM patients. Taken together, our findings describe novel dual roles of LMO2 to induce tumorigenesis and angiogenesis, and provide potential therapeutic targets in GBMs.
Cell Death and Differentiation (2015) **22,** 1517–1525; doi:10.1038/cdd.2015.7; published online 27 February 2015

Glioblastoma (GBM) is the most frequent and lethal primary brain tumor with inevitable recurrence in the vast majority of cases after conventional therapy.[1] Therefore, there is an urgent need to develop novel therapeutic options that effectively target therapy-resistant GBM cells. Cancer stem cells in GBM (glioma stem cells: GSCs) are a subpopulation of tumor cells that retains undifferentiated stem cell characteristics (stemness) and high tumorigenic potential.[2] Evidence is accumulating that GSCs drive GBM initiation and propagation and contribute to the development of resistance to current treatment options.[3–6] Therefore, this provides a novel therapeutic rationale for targeting GSC in GBM. However, the clinical significance of GSCs is still controversial and the regulatory molecular mechanisms for GSCs remain elusive.

The *LMO2* gene contains two zinc-binding LIM-domains that are essential for LMO2 as a bridging molecule in multiprotein complexes.[7] Through binding of the LIM domain to various proteins including TAL/SCL, GATA-1, E47, and LDB1, they are able to regulate gene expression at the transcriptional level by recognizing a unique bipartite DNA sequence comprising an E box separated by about one helix turn from a GATA site.[8]

Transcriptional dysregulation of *LMO2* is frequently observed in human acute T-cell lymphoblastic leukemia patients.[9] *Lmo2* transgenic activation in the thymus results in T-cell lymphoma/leukemia. Lmo2 overexpression in T-cell progenitors caused differentiation block, exit from quiescence, and increased self-renewal, all of which are the hallmarks of hematopoietic stem cells (HSCs).[10] Indeed, *Lmo2*-expressing T-cell progenitors display an HSC-like transcriptional signature indicating de-differentiation. This reprogramming event caused by *Lmo2* may indicate that LMO2 is a driver of cancer initiation in T-cell progenitors.

Despite these intensive studies of LMO2 in leukemia genesis in the past decade, pathophysiology of LMO2 in solid cancers remains largely undetermined. In this study, we

[1]School of Life Sciences and Biotechnology and Institute of Life Science and Natural Resources, Korea University, Seoul 136-713, Republic of Korea; [2]Department of Neurological Surgery, The Ohio State University, Columbus, OH 43210, USA; [3]Department of Cellular and Molecular Medicine, Lerner Research Institute, Cleveland Clinic, Cleveland, OH 44195, USA; [4]Department of Stem Cell Biology and Regenerative Medicine, Lerner Research Institute, Cleveland Clinic, Cleveland, OH 44195, USA; [5]Department of Molecular Biosciences, University of Texas at Austin, Austin, TX 78712, USA; [6]Specific Organs Cancer Branch, Research Institute and Hospital, National Cancer Center, Goyang 410-769, Republic of Korea; [7]Department of Molecular and Cellular Oncology, The University of Texas MD Anderson Cancer Center, Houston, TX 77030, USA; [8]Department of Molecular Virology, Immunology and Medical Genetics, The Ohio State University, Columbus, OH 43210, USA; [9]Department of Otorhinolaryngology-Head and Neck Surgery, Research Institute of Medical Science, Konkuk University School of Medicine, Seoul 143-752, Republic of Korea; [10]Department of Molecular Medicine, Cleveland Clinic Lerner College of Medicine, Cleveland, OH 44195, USA; [11]Case Comprehensive Cancer Center, Cleveland, OH 44195, USA and [12]James Comprehensive Cancer Center, The Ohio State University, Columbus, OH 43210, USA

*Corresponding authors: I Nakano, Department of Neurological Surgery, The Ohio State University, 410 w 12th avenue, Columbus 43210, OH, USA. Tel: +1 614 292 0358; Fax: +1 614 688 4882; E-mail: Ichiro.Nakano@osumc.edu

or H Kim, School of Life Sciences and Biotechnology and Institute of Life Science and Natural Resources, Korea University, Seoul 136-713, Republic of Korea. Tel: +82 2 3290 3059; Fax: +82 2 3290 3040; E-mail: hg-kim@korea.ac.kr

Abbreviations: GBM, glioblastoma; GFAP, glial fibrillary acidic protein; GSCs, glioma stem cells; HSCs, hematopoietic stem cells; LMO2, Lim domain only 2; NBE, neurobasal medium

Received 26.6.14; revised 30.12.14; accepted 14.1.15; Edited by R De Maria; published online 27.2.15

sought to elucidate the physiological roles and mechanism of action of LMO2 in GBM and GSCs in mice and human.

Results

LMO2 is required for GSC growth both *in vitro* and *in vivo*. First, we investigated the expression of LMO2 in GSC and non-GSC derived from acutely dissociated primary xenografts propagated *in vivo* sorted for CD133-positive and -negative population. Real-time PCR and western blot analysis demonstrated that LMO2 expression was reduced, whereas an astrocyte differentiation marker, glial fibrillary acidic protein was increased in the non-GSCs in Figure 1a. Human GBM-derived GSCs showed significant decline of *LMO2* expression upon induction of differentiation with serum-containing media (Supplementary Figure 1a). Transcriptome microarray data with 11 GCS samples and 5 normal astrocyte samples from Mao data set demonstrated that human GSCs have relatively higher *LMO2* mRNA expression compared with differentiated normal astrocytes (Figure 1b). Elevated LMO2 expression in GSCs was also observed in two other data set (Schulte data set and Lee data set; Figure 1c and Supplementary Figure 1b). Among the two GSC subtypes, *LMO2* expression was specifically higher in proneural subtype than mesenchymal one in both Mao data set and Bhat data set (Figure 1d). Altogether, LMO2 expression is enriched in GSCs with proneural identity. We then performed LMO2 knockdown by five different shLMO2 lentivirus clones in GSCs and selected the shLMO2 #5 with 90% reduction of LMO2 for the further study (Supplementary Figure 2a and b). *In vivo* limiting dilution assay shows that *LMO2* depletion attenuated sphere-forming activity in GSC1T (Figure 1e and Supplementary Figure 2c). Conversely, *LMO2* overexpression exhibited increased sphere-forming activity in the non-GSC, U87MG (Supplementary Figure 2d and e). These *in vitro* data appeared relevant *in vivo*, as the orthotopic mouse xenograft assays revealed that tumor growth of human GSCs is significantly diminished by *LMO2* knockdown (Figure 1f).

LMO2 is sufficient to induce glioma stemness from premalignant astrocytes both *in vitro* and *in vivo*. Next we investigated the phenotypic consequences of Lmo2 overexpression in primary premalignant astrocytes derived from *Ink4a/Arf* null mice (hereby termed as *Ink4a/Arf*$^{-/-}$ astrocytes), which lack p16^{Ink4a} and p19^{Arf} genes—the most frequently altered tumor suppressor genes in human GBM.[13] Overexpression of *Lmo2* increased *in vitro* growth of *Ink4a/Arf*$^{-/-}$ astrocytes (Figure 2a). This increase of cell growth by Lmo2 overexpression was associated with elevated expression of CyclinD1 protein (Figure 2b). Consistent with these *in vitro* data, Lmo2 overexpression significantly accelerated *in vivo* growth of subcutaneous and intracranial mouse tumors derived from *Ink4a/Arf*$^{-/-}$ astrocytes (Figure 2c). Notably, *Lmo2*- *Ink4a/Arf*$^{-/-}$ astrocytes-derived tumors have

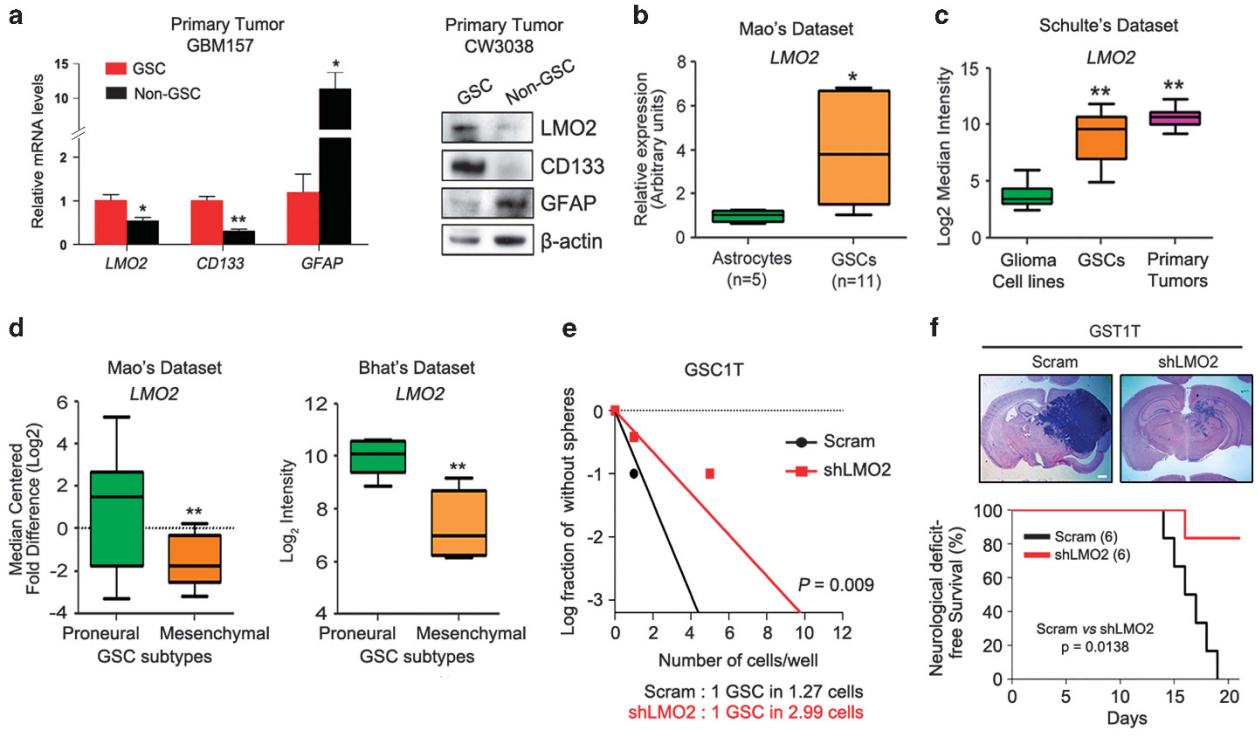

Figure 1 LMO2 is necessary for human glioma stem cell growth *in vivo* (**a**) mRNA and protein expression of LMO2, CD133, and glial fibrillary acidic protein (GFAP) in GSC and non-GSC acutely isolated from two different GBM-derived xenograft brain tumors based on the CD133 expression. (**b** and **c**) Relative *LMO2* mRNA expression in indicated samples in Mao's data set (**b**) and Schulte's data set (**c**). (**d**) Relative *LMO2* expression in proneural and mesenchymal GSC samples in indicated data set. (**e**) *In vitro* limiting dilution assays (LDAs) to determine the effect of shLMO2 on self-renewal activity in GSC1T cells. Wells without sphere formation were counted. $P = 0.009$ with extreme LDA (ELDA) analysis; http:// bioinf.wehi.edu.acu/software/elda/. (**f**) Representative H&E staining of whole-mouse brain xenografts derived from Scram- and shLMO2-GSCs (GST1T) and the Kaplan–Meier survival analysis. Scale bar represents 500 μm. Asterisk (*) indicates statistical significance by Student's *t*-test. *$P<0.05$; **$P<0.01$

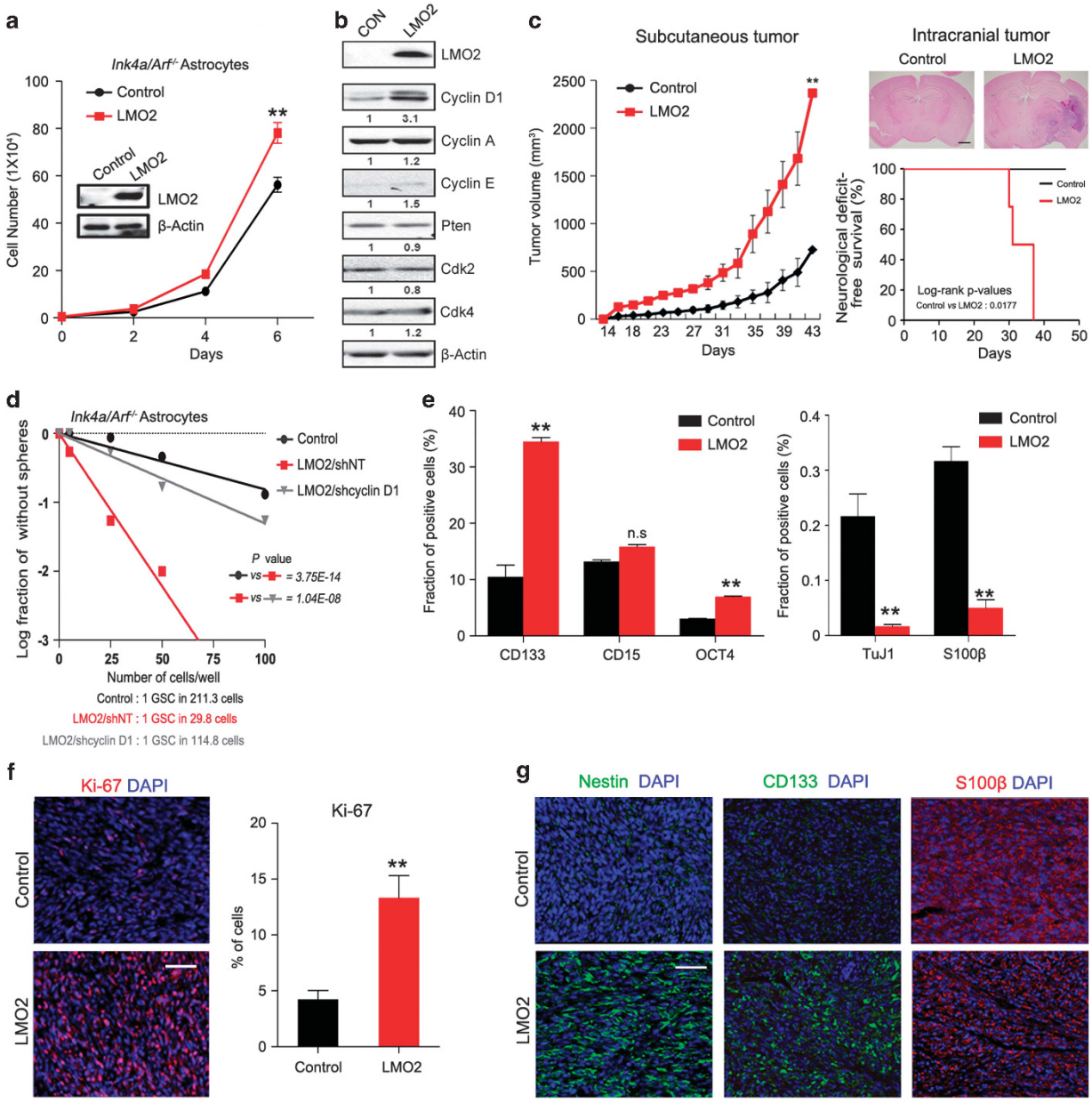

Figure 2 LMO is sufficient to induce stem cell phenotype in mouse premalignant astrocytes *in vivo* (**a**) Cell proliferation of Control-, and *Lmo2*-overexpressing *Ink4a/Arf*$^{-/-}$ astrocytes *in vitro*. Western blot showing the expression level of LMO2 in each sample. β-actin as internal control. (**b**) Protein expression levels of cell cycle-associated proteins in indicated samples. (**c**) An *in vivo* mouse subcutaneous ($n=6$ per group, left panel) and intracranial ($n=4$ per group, right upper panel) tumorigenic potential of Control- and *Lmo2-Ink4a/Arf*$^{-/-}$ astrocytes. Kaplan–Meier analysis of neurological deficit-free survival for the Lmo2 overexpression compared with the control (right lower panel). Scale bar represents 500 μm. (**d**) *In vitro* limiting dilution assay of Control-, *Lmo2*-, and *Lmo2/shCyclin D1- Ink4a/Arf*$^{-/-}$ astrocytes. (**e**) Proportion of CD133(+), CD15(+), OCT4(+), TuJ-1(+), and S100β(+) cells of Control- and *Lmo2-Ink4a/Arf*$^{-/-}$ astrocytes. (**f**) Representative immunofluorescence images and quantification of Ki-67 in subcutaneous tumors derived from Control- and *Lmo2-Ink4aArf*$-/-$ astrocytes. (**g**) Representative immunofluorescence images of Nestin, CD133, and S100β expression in subcutaneous tumors derived from Control- and *Lmo2-Ink4aArf*$-/-$ astrocytes. DAPI for nuclear staining. Scale bars represent 100 μm. Data are expressed as mean $\pm$ S.D. $^{**}P<0.01$

been shown to have histological features of high-grade glioma, such as intratumoral hemorrhage, angiogenesis, and necrosis (Supplementary Figure 3).

Because Lmo2 promotes self-renewal of preleukemic thymocytes,[10] we investigated if Lmo2 overexpression leads to stem cell phenotypes in brain cancers. When we performed *in vitro* limiting dilution assay, *Lmo2*-overexpressing *Ink4a/Arf*$^{-/-}$ astrocytes promotes sphere-forming cells that are markedly decreased by *Cyclin D1* knockdown, suggesting *Cyclin D1* is involved in Lmo2 mediated self-renewal activity (Figure 2d). With regard to the marker expression, *Lmo2*-overexpressing cells displayed a marked increase of stem cell marker, CD133;[14] 8% *versus* 35%, and OCT4; 3% *versus* 7% of CD133(+) cells in control *versus* *Lmo2*-ovexpressing cells as determined by FACS analysis (Figure 2e). In turn, expression of the differentiation markers, TuJ1 and S100β,

was strongly decreased in *Lmo2*-overexpressing cells. Consistent with these *in vitro* data, immunohistochemistry demonstrated increases of Ki-67, Nestin(+), and CD133(+) cells in *Lmo2*-overexpressing subcutaneous mouse tumors (Figure 2f and g). On the other hand, these tumors diminished the proportion of S100*β*(+) cells (Figure 2g). Taken together, Lmo2 promotes tumor propagation by inducing undifferentiated stem cell phenotype of *Ink4a/Arf*$^{-/-}$ astrocytes.

LMO2 mediates GSC phenotype through transcriptional regulation of the Jagged1-Notch signaling axis. Previously we identified that the key signaling pathways activated in proneural GSCs include Notch-, Shh-, and Wnt-mediated pathways.[12] Given that LMO2 is highly expressed in proneural but not mesenchymal GSCs (Figure 1d), we analyzed the effect of *LMO2* on these signaling pathways using luciferase reporter vectors containing the specific binding sequences of either CSL (Notch signaling), Gli-1 (Shh signaling), or TCF/LEF (TOP; Wnt/*β*-catenin signaling). Lmo2 overexpression resulted in a 1.8-fold increase of the CSL/Notch-responsive promoter activity (Figure 3a). Quantitative RT-PCR revealed that one of the Notch ligands, *Jagged1*, is upregulated in *Lmo2-Ink4a/Arf*$^{-/-}$ astrocytes (Figure 3b). *Jagged1* promoter region has one E-box (CANNTG) DNA motif that is known as a binding site for the LMO2 transcriptional complexes.[15] Indeed, *Lmo2* increased Jagged1 promoter activity in a dose-dependent manner (Figure 3c), and Jagged1 protein and cleaved Notch1 (Notch intracellular domain-NICD; Figure 3d and Supplementary Figure 4a). *Lmo2* also increased Notch downstream target genes *Hes1* and *Hey1*, and these increases were completely attenuated by shRNA-mediated depletion of *Jagged1* (Figure 3e and Supplementary Figure 4b). In turn, depletion of *LMO2* by shRNA greatly reduced Jagged1 expression in human GSCs (Figure 3f). *LMO2* expression in GSCs exhibited statistically significant positive correlation with those of *Jagged1, Hes1, Hey1*, and *Hey2* (Supplementary Figure 5). In addition, a gene set enrichment analysis (GSEA) of transcriptome in GBM patients exhibited a significant correlation between *LMO2* and *NOTCH* target gene signature (Figure 3g). The sphere-forming ability of *Lmo2-Ink4a/Arf*$^{-/-}$ astrocytes was completely attenuated by Jagged1 depletion (Figure 3h and Supplementary Figure 6). Collectively, these data indicate that LMO2 causally contributes to the reprogramming of differentiated astrocytes into GSC-like tumorigenic cells in a Jagged1/Notch pathway-dependent manner.

LMO2 induces endothelial-like cells from GSCs. Next, we investigated the cellular identities of xenografted human GSCs in mouse brains by using a GFP-labeled GSC sample (GFP$^+$ GSC1T). With a close investigation at the perivascular area in tumors, we identified vWF(+) cells contained either GFP(+) or (−) cells (Figure 4a), raising a possibility that tumor vasculature is composed of both host endothelial cells and GSC-derived cells that utilize vascular mimicry.[16] Given that LMO2 is widely expressed in the vasculature of a variety of neoplasm,[17] we sought to determine whether the LMO2-driven tumorigenicity is associated with facilitated angiogenesis in an autocrine or paracrine manner. To assess the paracrine effect, we treated human umbilical vein endothelial cells (HUVECs) with the conditioned medium derived from *Lmo2*-overexpressing cells under the endothelial cell growth-promoting culture condition. This treatment did not exhibit any significant changes in *in vitro* tube formation, suggesting that *Lmo2* may not be involved in angiogenic induction in a paracrine manner (Figure 4b and Supplementary Figure 7a). Next, we directly induced tube formation of Control- and *Lmo2-Ink4a/Arf*$^{-/-}$ astrocytes using the same culture condition. Lmo2 overexpression markedly increased the tube-like structure in an eightfold in *Ink4a/Arf*$^{-/-}$ cells compared with the control (Figure 4b and Supplementary Figure 7b). Furthermore, this phenotypic change by *Lmo2* transduction was associated with enhanced immunoreactivity to two endothelial-specific markers, VEGFR2 and VE-cadherin (Figure 4c). Quantitative analysis by FACS showed the increases of VEGFR2, VE-cadherin, and CD34 were greater than sixfold (Figure 4d). Consistent with these mouse data, *LMO2* knockdown in human primary GSCs (GSC1T) significantly reduced the number of tubes along with the decreased expression of *VE-cadherin* and *VEGFR2 in vitro* (Figure 4e,Supplementary Figure 7c and d). Furthermore, *LMO2* knockdown in GFP-expressing human GSC1T brain xenografts resulted in a fivefold decrease in vWF-expressing GFP(+) cells compared with the control tumors (Figure 4f). In turn, Lmo2 overexpression displayed a substantial increase of vWF(+) cells in *Lmo2-Ink4a/Arf*$^{-/-}$ astrocytes-derived mouse tumors (Figure 4g).

We next performed chromatin immunoprecipitation assay to determine whether LMO2 directly occupies the promoter regions of the *VE-cadherin* gene. Both of the two VE-cadherin promoter regions were significantly amplified by quantitative PCR from chromatin immunoprecipitated *Ink4a/Arf*$^{-/-}$ astrocyte samples using LMO2 antibody in the proangiogenic condition (EGM2 media; Figure 4h). Collectively, these data indicate that LMO2 binds and activates the promoter regions of the *VE-cadherin* gene thereby promoting endothelial-like cells from mouse premalignant astrocytes and human GSCs both *in vitro* and *in vivo*.

VE-cadherin(+) cells derived from GSCs promotes tumor aggressiveness. We then sought to determine whether the human GSC-derived VE-cadherin(+) cells contribute to tumor growth *in vivo* (Figure 5). To this end, we transplanted GSCs after infection with a lentiviral vector containing the herpes simplex virus thymidine kinase gene (*tk*) under the control of transcriptional regulatory elements of the *VE-cadherin* gene (VE-cadherin-*tk*) so that the GSC-derived VE-cadherin(+) cells would be selectively eradicated by ganciclovir. The ganciclovir treatment markedly diminished the vWF(+) cell population in VE-cadherin-*tk* expressing mouse tumors but not in the negative control tumors (Figure 5a). As a positive control (PGK-*tk*), we validated the cytotoxic effect of ganciclovir in PGK-*tk* expressing tumors. Consequently, elimination of GSC-derived VE-cadherin-expressing cells resulted in a statistically significant survival benefit for mice bearing GBM-like tumors derived from GSCs (Figure 5b).

Clinical relevance of LMO2 as a therapeutic target in GBM. Last, we examined the clinical relevance of these

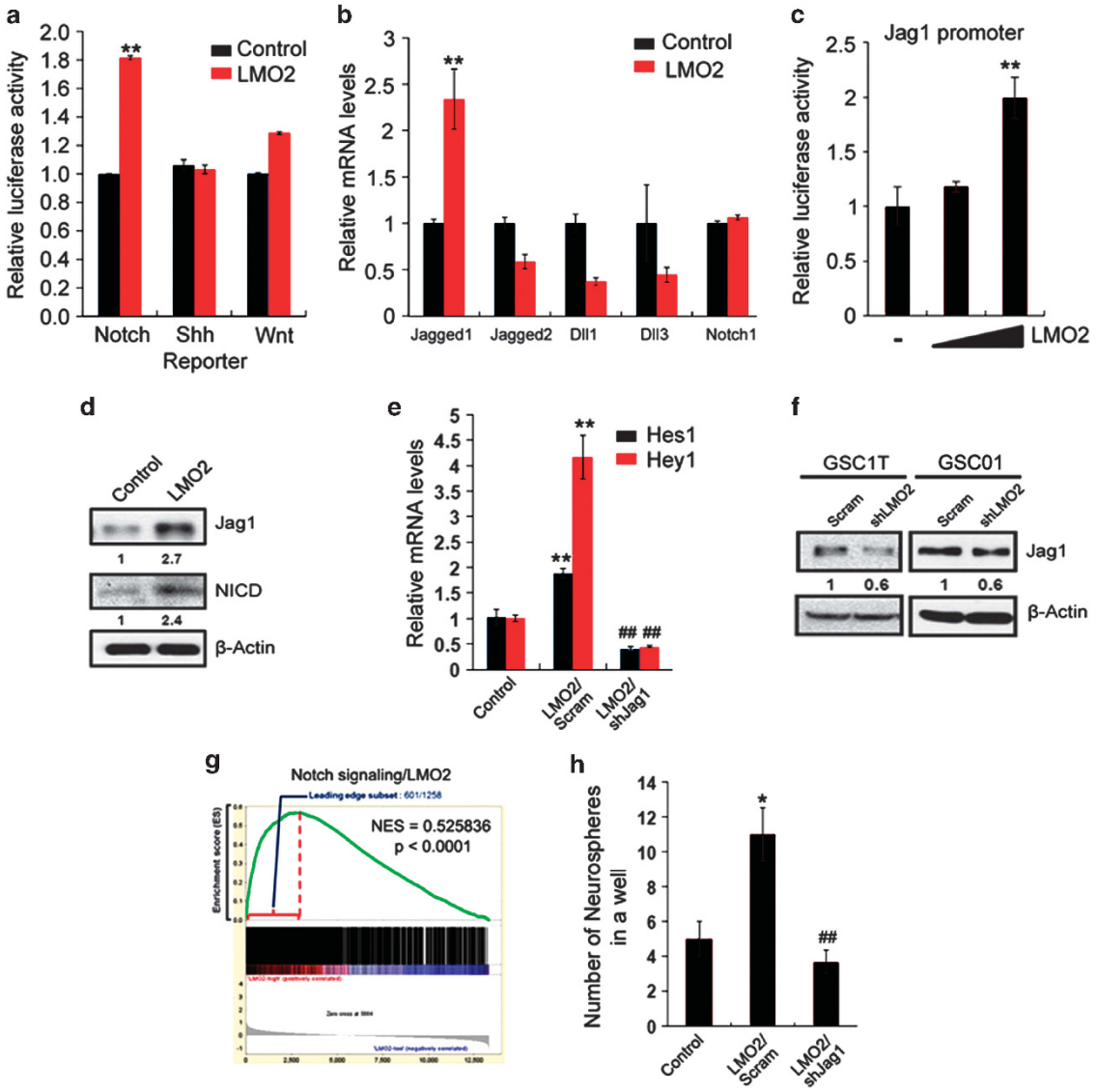

Figure 3 LMO2 maintains stem cell phenotypes by transcriptional activation of Jagged1-Notch signaling pathway (**a**) Relative activity of Notch (CLS), Shh (GLI-1), and Wnt (TCF-LEF) responses element luciferase reporters. (**b**) Relative mRNA levels of *Jagged1*, *Jagged2*, *Dll1*, *Dll3*, and *Notch1*. (**c**) The effect of LMO2 overexpression on the *Jagged1* promoter-driven luciferase activity. Rectangle indicates increasing doses of the LMO2 expressing vector. (**d**) Western blot showing expression levels of Jagged1 and active Notch1 (NICD) proteins in indicated samples. (**e**) *Hes1* and *Hey1* mRNA levels of Control-, *Lmo2*-, and *Lmo2*-shJagged1-*Ink4a/Arf*$^{-/-}$ astrocytes. (**f**) Jagged1 protein levels in 2 GSC samples with or without LMO2 silencing (shLMO2). (**g**) GSEA analysis showing the high enrichment of Notch target gene signature in LMO2-overexpressng tumors. (**h**) The numbers of neurosphere forming cells in indicated samples. Data are mean ± S.D. $^{*}P<0.05$, $^{**}P<0.01$, $^{\#\#}P<0.01$

experimental data by using the glioma tumor samples. In order to do that, we interrogated tissue microarray of 93 clinical glioma samples containing WHO grade II–IV tumors, as well as adjacent normal brain tissues to determine its expression and a potential contribution of LMO2 to the patient survival. Immunohistochemistry displayed significantly higher LMO2 protein expression in high-grade glioma tissues compared with low-grade glioma tissues (Figure 6a and Supplementary Figure 8a). Furthermore, the expression of LMO2 is correlated with poor GBM patient survival (Supplementary Figure 8b). Among the 4 LMO genes, *LMO2* was significantly elevated in astrocytoma, oligodendrocytoma, and GBM compared with nontumor tissues as analyzing by the Repository of Molecular Brain Neoplasia Data (REMBRANT) and Grzmil's data set (Figure 6b and Supplementary Figure 8c). Significant elevation of LMO2 expression in GBM tumors compared with lower grade glioma tissues was also confirmed with two different data set (Phillips and Freije; Figure 6c). When GBM patients were separated based on the prognosis (cut off: 3-year survival), those with shorter survival had significantly elevated LMO2 expression (Figure 6d). This trend was also confirmed by the Kaplan–Meier survival analysis (Figure 6e and Supplementary Figure 7d; REMBRANT survival data). Interestingly, higher LMO2 levels were also strongly correlated with patient clinical characteristics such as age (>40 years), histopathological grade (WHO grade

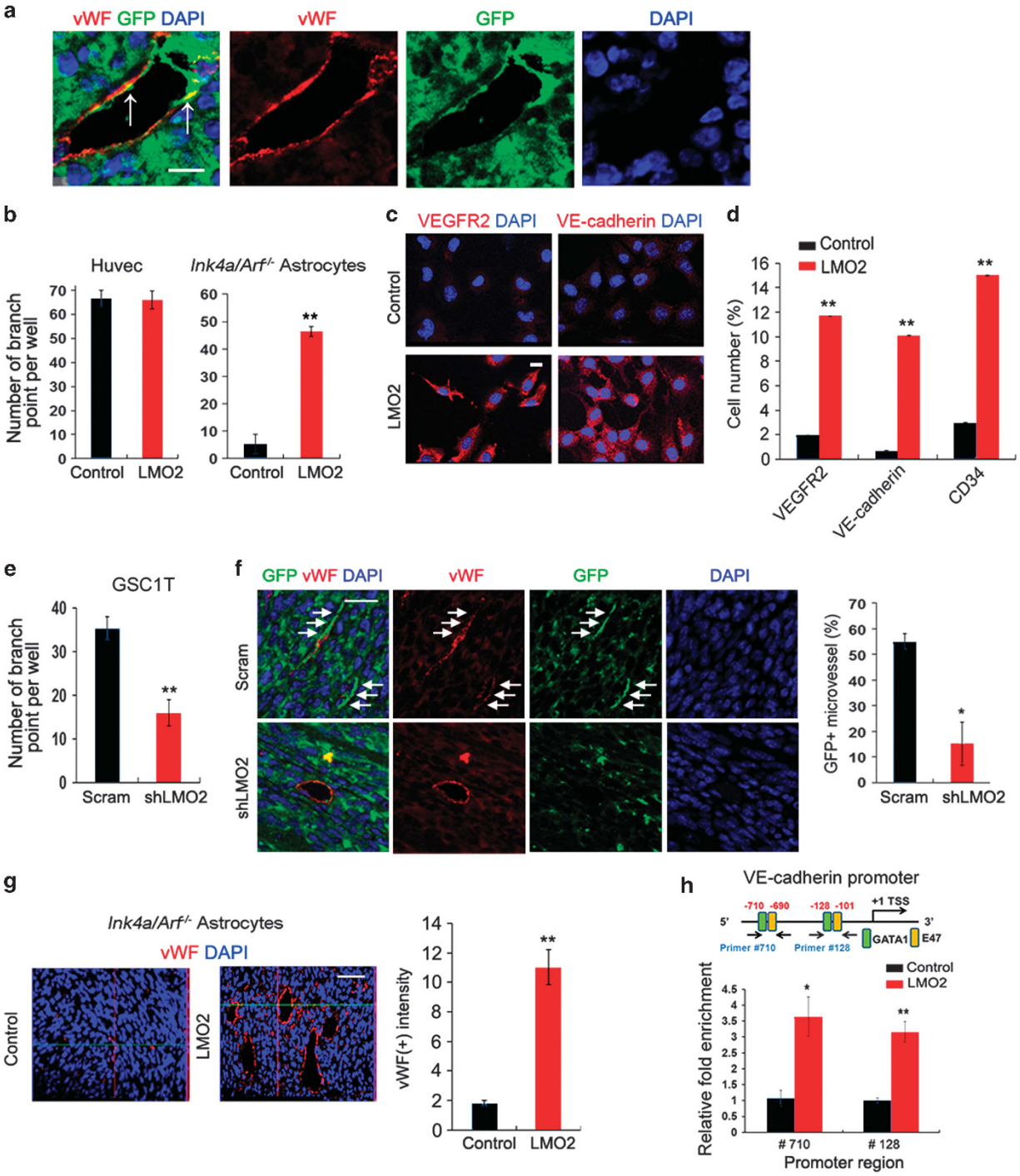

Figure 4 LMO2 modulates endothelial-like cell conversion of GSCs *in vivo* (**a**) Representative images of vWF and GFP in GFP expressing GSC-derived mouse brain tumors. DAPI for nuclear staining. Arrows indicate double-positive cells for GFP and vWF at perivascular area. Scale bar represents 10 μm. (**b**) Effects of conditioned media from control- and *Lmo2-Ink4a/Arf*$^{-/-}$ astrocytes on tube formation of HUVEC cells (left panel). Effect of Lmo2 overexpression on tube formation of *Ink4a/Arf*$^{-/-}$astrocytes (right panel). (**c**) Immunofluorescence showing VE-cadherin and VEGFR2 expressions in indicated samples. Scale bar represents 10 μm. (**d**) FACS data showing the proportions of VE-cadherin(+), VEGFR2(+), and CD34(+) cells in the control- and *Lmo2-Ink4a/Arf*$^{-/-}$ astrocytes grown in the proangiogenic media. (**e**) An *in vitro* tube forming ability of indicated samples. (**f**) GFP/vWF double-positive cells in GFP-labeled GSCs (GSC1T) brain xenografts with indicated treatments. Arrow indicates GFP/vWF double-positive cells. Graph in right panel indicates quantification. DAPI for nuclear staining. Scale bar represents 20 μm. (**g**) Representative images and quantification of the vWF(+) cells in Control- and *Lmo2-Ink4a/Arf*$^{-/-}$ tumors. Scale bar represents 50 μm. (**h**) The occupancy of *LMO2* to the cognate binding elements in the VE-cadherin promoter in *Ink4a/Arf*$^{-/-}$ astrocytes. Data are mean ± S.D. **P*<0.05, ***P*<0.01

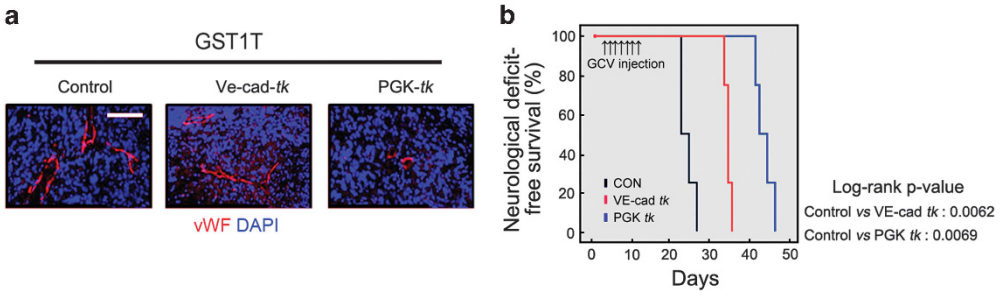

Figure 5 VE-cadherin(+) cells derived from human GSC1T give rise to endothelial-like cells and has a role in tumor growth *in vivo* (**a**) Immunofluorescence displaying vWF-expressing cells (red) in ganciclovir-treated mouse xenograft brain tumors derived from GST1T with indicated lentiviral infection. DAPI for nuclear staining. Scale bar represents 50 μm. (**b**) Kaplan–Meier curves showing the tumor-free survival of indicated tumor burden mice ($n = 4$ mice/group) after ganciclovir treatment (arrows)

IV), and clinical status of affected patients (<80% Karnofsky performance score; Supplementary Table 1). Collectively, *LMO2* is a clinically relevant molecular target in GBM.

Discussion

The significance of this study is related to our identification of a novel function of LMO2 in GBMs and GSCs. LMO2 promotes cell proliferation and the gain of cancer stem cell phenotypes via the Jagged1-Notch signaling axis. LMO2 also facilitates endothelial-like cell conversion of GSCs by the direct transcriptional activation of VE-cadherin. Therefore, the mechanism of LMO2 action may be dependent upon spatial and cellular context. LMO2, in particular under proangiogenic conditions, resulted in endothelial cell marker expression along with subsequent endothelial-like cell conversion of GSCs. In these conditions, LMO2 might comprise a transcriptional complex with TAL-1, E47, LMO2, GATA-2, and LDB1 to regulate VE-cadherin in agreement with a previous study with HUVEC cells.[18] In erythroid cells, LMO2 is known to bind to basic-helix-loop-helix transcription factors including TAL1/SCL, LDB1, and GATA-1, thereby forming a large DNA-binding complex to drive the downstream target signals.[8] An open question still remains as to how LMO2 coordinates to form a transcrption factor complex in order to mediate the tumorigenic activity of GSCs. Such candidates include Olig2, which is highly expressed in proneural GBM and has a critical role in maintaining stem cell phenotypes in GSCs.[19,20] In support of this hypothesis, several reports have shown a striking correlation between *LMO2, TAL1*, and *Olig2* based on gene expression analysis in human and murine T-cell leukemia.[21–23] In future studies, it will be interesting to explore whether LMO2 interacts with Olig2 to regulate GSCs and brain tumorigenesis.

Presence of tumor-derived vascular components sheds light on the plasticity of cancer cells and the potential involvement of cancer stem cells in cancer-associated angiogenesis. In normal brains, *Lmo2* is highly expressed in mouse vascular endothelium and is necessary for angiogenic remodeling of the existing capillary network into mature vasculature.[17,24] GBMs display an enriched vasculature phenotype, which is strongly correlated with tumor aggressiveness and poor patient outcomes. Our studies presented the first evidence that LMO2 modulates endothelial-like cell conversion of GSCs by directly regulating VE-cadherin transcriptional activity. Prolonged survival of mice with the *VE-cadherin* promoter-driven Hsv *tk* suicide system further suggested the gain of the endothelial-like cell phenotype in GSCs might regulate tumor aggressiveness. Nonetheless, research on the contribution of GBM cells including GSCs to tumor angiogenesis is still evolving and many questions remain to be addressed. Recently, some studies demonstrated the evidence of transdifferentiation of some GSCs into endothelial cells, whereas others demonstrated that some GSCs are incapable of such transdifferentiation; instead they give rise to vascular stromal cells (e.g. smooth muscle cells, pericytes).[16,25–29] One possible explanation for this discrepancy is that the lineage specification may be linked to the GBM/GSC subtypes. Given that neural stem cells are known to transdifferentiate into endothelial cells,[30] the proneural GSC subtype may have the potential to give rise to endothelial cells rather than stromal cells. To investigate whether mesenchymal GSCs are capable of giving rise to stromal cells is also an interesting question for future studies.

In conclusion, in this study, we identified that LMO2 acts as an oncogenic transcription factor by maintaining the GSC phenotypes and inducing conversion of GSCs into endothelial-like cells. Collectively, our data provide a set of evidence suggestive of a novel signaling mechanism underlying the tumorigenic and angiogenic traits of GSCs to regulate tumor growth *in vivo*. Future characterization of the LMO2-mediated pathways could elucidate novel molecular mechanisms of contribution of GSCs toward GBM initiation and propagation, and eventually lead to development of novel and effective targeted therapies for this devastating disease.

Materials and Methods

Ethics. Experiments using human tissue-derived materials were carried out under the approved institutional review board at Korea University, the Cleveland Clinic, and Ohio State University (OSU). All animal experimentation was performed with the approval of the OSU Animal Research Committee, following NIH guidelines.

Patient-derived tissue culture. GBM tissue-derived neurosphere cultures (GSC1T, GSC01, GSC13, and GSC83), GBM157, and CW3038 were established and maintained in the Kim, the Nakano, the Lathia laboratory as previously described.[11,12] These GSCs were cultured in Neurobasal medium (NBE; Invitrogen, Carlsbad, CA, USA) supplemented with modified N2, B27, EGF (20 ng/ml; R&D Systems, Minneapolis, MN, USA) and bFGF (20 ng/ml; R&D Systems) in suspension or in an adherent culture with laminin-coated flasks.

Cell lines and reagents. Primary HUVECs were purchased from American Type Culture Collection. *Ink4a/Arf*$^{-/-}$ astrocytes were maintained in DMEM high glucose medium enriched with 10% fetal bovine serum (Hyclone, Logan, UT, USA). HUVECs and *Ink4a/Arf*$^{-/-}$ astrocytes were maintained in endothelial cell basal medium-2 with growth supplements (EGM2; Clonetics, San Diego, CA, USA).

***In vitro* tube formation assay.** *In vitro* tube formation of HUVECs, *Ink4a/Arf*$^{-/-}$ astrocytes, and GSCs was assessed using an *in vitro* angiogenesis assay kit (Chemicon, Temecula, CA, USA). Control- and *Lmo2-Ink4a/Arf*$^{-/-}$astrocytes were cultured for 24 h (5×10^5 cells/10-cm plate) and then used as a conditioned medium, which had been filtered through a 0.2-μm filter (Sartorius Stedim Biotech, Goettingen, Germany). Primary *Ink4a/Arf*$^{-/-}$astrocytes and HUVECs

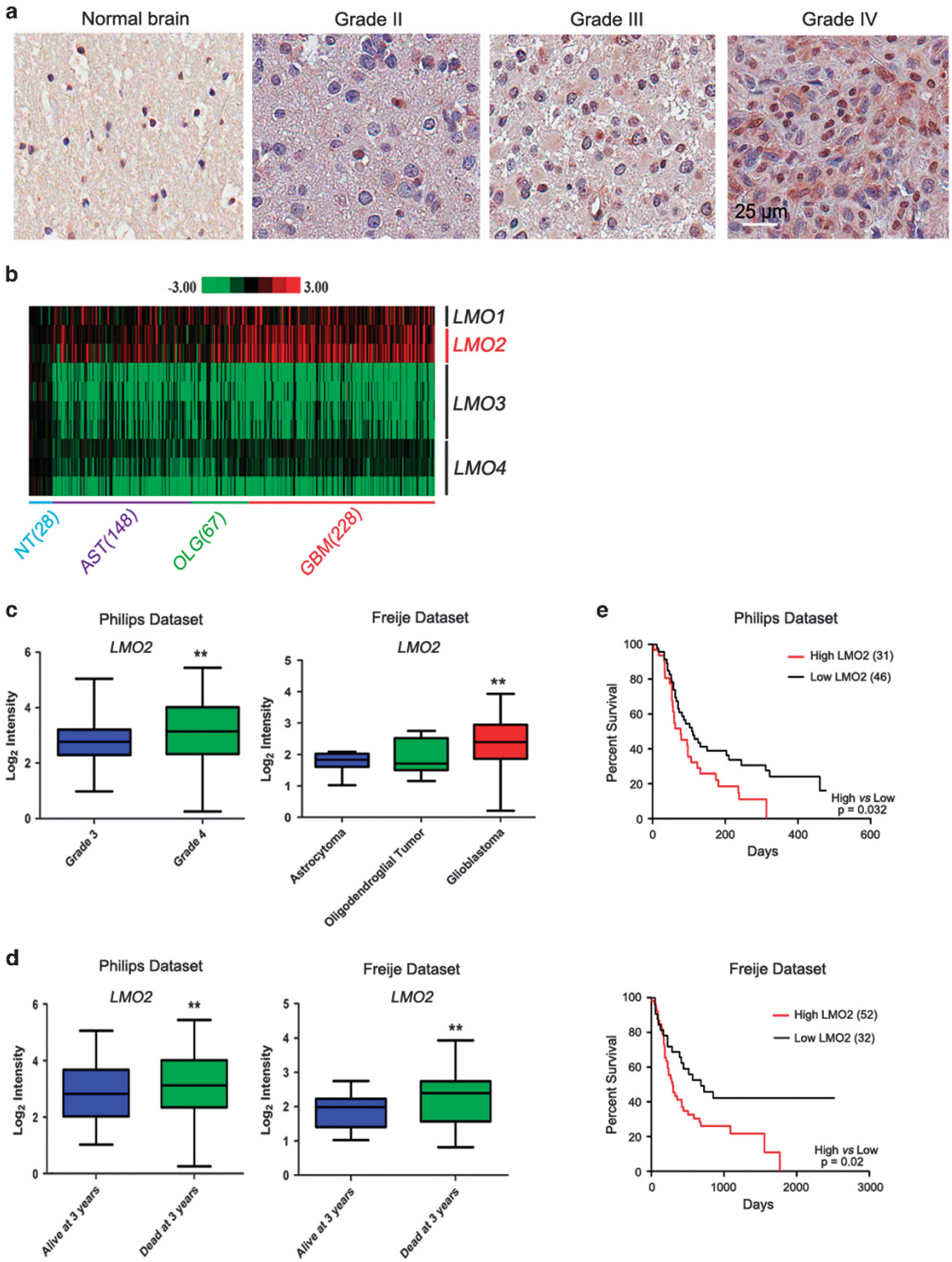

Figure 6 LMO2 is highly expressed in GBM and its expression is inversely correlated with post-surgical patient prognosis (**a**) Representative images of LMO2 immuohistochemistry in different WHO tumor grades of clinical glioma samples or normal brain tissues. (**b**) Heatmap analysis showing that elevated *LMO2* mRNA levels in high-grade brain tumors. NT, nontumor; AST, astrocytoma; OLG, oligodendrocytoma; GBM, glioblastoma. (**c** and **d**) Relative expression levels of *LMO2* in normal brain, astrocytoma, and glioblastoma in indicated patient groups in Phillips data set and Freije data set. (**e**) Kaplan–Meier survival analysis showing negative correlation of *LMO2* mRNA levels with patient survival. Asterisk (*) indicates statistical significance by Student's *t*-test. $^{**}P<0.01$

(1×10^4 cells/well in 96-well plate) were cultured in each type of conditioned medium at 37 °C. Six hours after incubation, the cultures were photographed (×40 magnification). Three random view-fields per well were examined, and tube numbers were counted.

Subcutaneous and orthotopic implantation assay. To establish subcutaneous xenograft models, cells (2×10^6) were subcutaneously injected into nude mice (BALB/c nu/nu mice). For the orthotopic implantation, 5×10^4 cells were stereotactically injected into the left striatum of nude mice (coordinates: anterior–posterior, +2 mm; medial–lateral, +2 mm; dorsal–ventral from the bregma, –3 mm from the dura). For ganciclovir treatment, mice received ganciclovir at 50 mg/kg intraperitoneally for 5 days. Ganciclovir-treated mice were monitored for survival and collected samples for histology and immunofluorescence.

Statistics. Data were analyzed by two-tailed Student's *t*-test. *P*-values <0.05 and <0.01 were considered statistically significant. The correlations between gene expression levels were evaluated by Spearman's rank correlation coefficient (ρ).

Other experimental materials and methods are detailed in Supplementary Materials and Methods.

Acknowledgements. We thank Drs Jeremy Rich at Cleveland Clinic, Hideyuki Saya at Keio University, Harley I. Kornblum at UCLA, and Antonio E. Chiocca at Brigham and Women's Hospital for constructive discussion and suggestions for this study. We also thank the members in the Kim and Nakano labs for constructive criticism for this paper. This work was supported in part by The American Cancer Society MRSG-08-108-01, NIH/NCI P01 CA163205, R21 CA175875, NIH/NINDS R01 NS083767, and R01 NS087913 (to IN); the National Research Foundation (NRF) of Korea grant funded by the Korean government (MEST; 2011-0017544, to HK); the Basic Science Research Program through the NRF of Korea (2011-0024089, to SHK); and the Institute of Life Science and Natural Resources grant of Korea University (to SO).

1. Wen PY, Kesari S. Malignant gliomas in adults. *N Engl J Med* 2008; **359**: 492–507.
2. Park DM, Rich JN. Biology of glioma cancer stem cells. *Mol Cells* 2009; **28**: 7–12.
3. Hambardzumyan D, Squatrito M, Holland EC. Radiation resistance and stem-like cells in brain tumors. *Cancer Cell* 2006; **10**: 454–456.
4. Rich JN. Cancer stem cells in radiation resistance. *Cancer Res* 2007; **67**: 8980–8984.
5. Frosina G. DNA repair and resistance of gliomas to chemotherapy and radiotherapy. *Mol Cancer Res* 2009; **7**: 989–999.
6. Schmalz PG, Shen MJ, Park JK. Treatment resistance mechanisms of malignant glioma tumor stem cells. *Cancers (Basel)* 2011; **3**: 621–635.
7. Rabbitts TH. LMO T-cell translocation oncogenes typify genes activated by chromosomal translocations that alter transcription and developmental processes. *Genes Dev* 1998; **12**: 2651–2657.
8. Wadman IA, Osada H, Grutz GG, Agulnick AD, Westphal H, Forster A *et al.* The LIM-only protein Lmo2 is a bridging molecule assembling an erythroid, DNA-binding complex which includes the TAL1, E47, GATA-1 and Ldb1/NLI proteins. *EMBO J* 1997; **16**: 3145–3157.
9. Van Vlierberghe P, van Grotel M, Beverloo HB, Lee C, Helgason T, Buijs-Gladdines J *et al.* The cryptic chromosomal deletion del(11)(p12p13) as a new activation mechanism of LMO2 in pediatric T-cell acute lymphoblastic leukemia. *Blood* 2006; **108**: 3520–3529.
10. McCormack MP, Young LF, Vasudevan S, de Graaf CA, Codrington R, Rabbitts TH *et al.* The Lmo2 oncogene initiates leukemia in mice by inducing thymocyte self-renewal. *Science* 2010; **327**: 879–883.
11. Jin X, Kim SH, Jeon HM, Beck S, Sohn YW, Yin J *et al.* Interferon regulatory factor 7 regulates glioma stem cells via interleukin-6 and Notch signalling. *Brain* 2012; **135**: 1055–1069.
12. Mao P, Joshi K, Li J, Kim SH, Li P, Santana-Santos L *et al.* Mesenchymal glioma stem cells are maintained by activated glycolytic metabolism involving aldehyde dehydrogenase 1A3. *Proc Natl Acad Sci USA* 2013; **110**: 8644–8649.
13. Cancer Genome Atlas Research NetworkComprehensive genomic characterization defines human glioblastoma genes and core pathways. *Nature* 2008; **455**: 1061–1068.
14. Singh SK, Hawkins C, Clarke ID, Squire JA, Bayani J, Hide T *et al.* Identification of human brain tumour initiating cells. *Nature* 2004; **432**: 396–401.
15. Ryan DP, Duncan JL, Lee C, Kuchel PW, Matthews JM. Assembly of the oncogenic DNA-binding complex LMO2-Ldb1-TAL1-E12. *Proteins* 2008; **70**: 1461–1474.
16. El Hallani S, Boisselier B, Peglion F, Rousseau A, Colin C, Idbaih A *et al.* A new alternative mechanism in glioblastoma vascularization: tubular vasculogenic mimicry. *Brain* 2010; **133**: 973–982.
17. Gratzinger D, Zhao S, West R, Rouse RV, Vogel H, Gil EC *et al.* The transcription factor LMO2 is a robust marker of vascular endothelium and vascular neoplasms and selected other entities. *Am J Clin Pathol* 2009; **131**: 264–278.
18. Deleuze V, El-Hajj R, Chalhoub E, Dohet C, Pinet V, Couttet P *et al.* Angiopoietin-2 is a direct transcriptional target of TAL1, LYL1 and LMO2 in endothelial cells. *PLoS One* 2012; **7**: e40484.
19. Verhaak RG, Hoadley KA, Purdom E, Wang V, Qi Y, Wilkerson MD *et al.* Integrated genomic analysis identifies clinically relevant subtypes of glioblastoma characterized by abnormalities in PDGFRA, IDH1, EGFR, and NF1. *Cancer Cell* 2010; **17**: 98–110.
20. Ligon KL, Huillard E, Mehta S, Kesari S, Liu H, Alberta JA *et al.* Olig2-regulated lineage-restricted pathway controls replication competence in neural stem cells and malignant glioma. *Neuron* 2007; **53**: 503–517.
21. Smith S, Tripathi R, Goodings C, Cleveland S, Mathias E, Hardaway JA *et al.* LIM domain only-2 (LMO2) induces T-cell leukemia by two distinct pathways. *PLoS One* 2014; **9**: e85883.
22. Dave UP, Akagi K, Tripathi R, Cleveland SM, Thompson MA, Yi M *et al.* Murine leukemias with retroviral insertions at Lmo2 are predictive of the leukemias induced in SCID-X1 patients following retroviral gene therapy. *PLoS Genet* 2009; **5**: e1000491.
23. Ferrando AA, Neuberg DS, Staunton J, Loh ML, Huard C, Raimondi SC *et al.* Gene expression signatures define novel oncogenic pathways in T cell acute lymphoblastic leukemia. *Cancer Cell* 2002; **1**: 75–87.
24. Yamada Y, Pannell R, Forster A, Rabbitts TH. The oncogenic LIM-only transcription factor Lmo2 regulates angiogenesis but not vasculogenesis in mice. *Proc Natl Acad Sci USA* 2000; **97**: 320–324.
25. Ricci-Vitiani L, Pallini R, Biffoni M, Todaro M, Invernici G, Cenci T *et al.* Tumour vascularization via endothelial differentiation of glioblastoma stem-like cells. *Nature* 2010; **468**: 824–828.
26. Wang R, Chadalavada K, Wilshire J, Kowalik U, Hovinga KE, Geber A *et al.* Glioblastoma stem-like cells give rise to tumour endothelium. *Nature* 2010; **468**: 829–833.
27. Ping YF, Bian XW. Consice review: contribution of cancer stem cells to neovascularization. *Stem Cells* 2011; **29**: 888–894.
28. Soda Y, Marumoto T, Friedmann-Morvinski D, Soda M, Liu F, Michiue H *et al.* Transdifferentiation of glioblastoma cells into vascular endothelial cells. *Proc Natl Acad Sci USA* 2011; **108**: 4274–4280.
29. Cheng L, Huang Z, Zhou W, Wu Q, Donnola S, Liu JK *et al.* Glioblastoma stem cells generate vascular pericytes to support vessel function and tumor growth. *Cell* 2013; **153**: 139–152.
30. Wurmser AE, Nakashima K, Summers RG, Toni N, D'Amour KA, Lie DC *et al.* Cell fusion-independent differentiation of neural stem cells to the endothelial lineage. *Nature* 2004; **430**: 350–356.

Supplementary Information accompanies this paper on Cell Death and Differentiation website (http://www.nature.com/cdd)